

Article

Study on the Influence of Electron Beam Radiation Sterilization Method on Chinese Mural Pigment

Min Luo ^{1,†}, Peng Bo ^{1,2,†}, Yang Shao ¹, Zhiming Liu ², Diandou Xu ^{1,*} and Lingling Ma ^{1,*}

¹ Beijing Engineering Research Center of Radiographic Techniques and Equipment, Institute of High Energy Physics, Chinese Academy of Sciences, Beijing 100049, China

² State Key Laboratory of Chemical Resource Engineering, Beijing University of Chemical Technology, Beijing 100029, China; liuzm@mail.buct.edu.cn

* Correspondence: xudd@ihep.ac.cn (D.X.); malingling@ihep.ac.cn (L.M.); Tel.: +86-010-88236403 (L.M.)

† These authors contributed equally to this work.

Abstract: Murals are one of the important cultural heritages of mankind. The microbial control of murals is an important subject in mural painting conservation. In recent years, electron beam radiation sterilization has attracted more and more attention in the field of cultural relic protection. Murals are immovable cultural relics, so conventional electron beam irradiation equipment can not be used. However, the development of small mobile electron beam irradiation equipment shows the potential of radiation's application in the sterilization protection of immovable cultural relics such as murals. A feasibility study of radiation sterilization in mural paintings is needed to investigate the effect of sterilization and the influence of sterilization dose on the stability of mural painting pigments and bonding materials. In this paper, the radiation effects of typical bacteria in tomb murals and mineral pigment powder in ancient Chinese paintings were studied in a laboratory. Firstly, *aeromonas hydrophila* (*Aer.h*) and *penicillium flavigenum* (*PNC*) were selected as representative strains to determine the appropriate sterilization dose for murals. Then, the effects of radiation on seven kinds of ancient Chinese mineral pigments and white calcium carbonate in the ground layer were verified. The results are as follows: the radiation dose of 10 kGy can effectively remove the two typical strains. This sterilization dose will cause a color difference in calcium carbonate and lead white, while other color pigments are essentially stable. Based on the color difference and UV-vis intensities of the four white carbonate samples, the color change in two of them increased with increasing the dose up to 30 kGy, after which signs of saturation began to appear. X-ray diffraction (XRD), Raman spectra, X-ray photoelectron spectroscopy (XPS) and X-ray absorption near edge structure (XANES) spectra showed that the chemical structure of the samples did not change after irradiation. The formation of free radicals in treated samples was confirmed using an electron paramagnetic resonance (EPR) spectrum test. According to all characterization results, the color difference between the four white carbonate samples may be due to the combination of unpaired electrons and defects in the process of electron beam irradiation to form color centers. After forming the color center, the light absorption of the four samples changed. This is a reversible change, but the samples will take a long time to return to their original state. This study focuses on the influence of electron beam radiation on pigment composition, which is a preliminary exploration of whether radiation sterilization can be applied to the protection of ancient Chinese mural paintings, and the experimental results can provide basic data for later application.



Citation: Luo, M.; Bo, P.; Shao, Y.; Liu, Z.; Xu, D.; Ma, L. Study on the Influence of Electron Beam Radiation Sterilization Method on Chinese Mural Pigment. *Processes* **2023**, *11*, 1403. <https://doi.org/10.3390/pr11051403>

Academic Editor: Maria Victoria Lopez-Ramon

Received: 9 April 2023

Revised: 28 April 2023

Accepted: 2 May 2023

Published: 5 May 2023



Copyright: © 2023 by the authors. Licensee MDPI, Basel, Switzerland. This article is an open access article distributed under the terms and conditions of the Creative Commons Attribution (CC BY) license (<https://creativecommons.org/licenses/by/4.0/>).

Keywords: electron beam radiation; mural protection; radiation sterilization; mineral pigment; chromatic aberration

1. Introduction

The biodegradable environment constantly affects the protection of interior painting cultural heritage, mainly represented by mural paintings [1]. With the development of

science and technology, researchers continue to optimize the protection methods of the microbial sterilization of cultural relics in order to minimize the side effects of the protection process in terms of the destruction of cultural relics and environmental pollution [2]. Microwave, plasma, irradiation and other physical sterilization methods have begun to be used in the field of cultural relic protection. Gamma radiation sterilization has been proven to be feasible in a variety of painting cultural heritage such as tempera painting [3,4] and oil on canvas [5], with good safety and effectiveness [4,6]. A dose of around 500 Gy can easily kill larvae, while fungi require 10 kGy [6,7]. For *Streptomyces* with high radiation resistance, a 25 kGy dose is sufficient for sterilization [4].

In the process of cultural relic color protection, effective sterilization is the basis, and the nondestructive evaluation of cultural relics can guide the application of technology. For example, as the most common painting cultural heritage in ancient China, mural paintings are composed of pigments, binders, plaster, etc. [8]. These organic or inorganic materials may exhibit obvious changes after irradiation. In order to investigate the possible color changes in pigments (mineral pigment) after radiation sterilization and irradiation, the changes were quantified according to standards published by the Commission Internationale de l'éclairage (CIE). Table 1 summarizes some of the ancient mineral pigments that have been irradiated and studied previously.

Table 1. Ancient mineral pigments used in irradiation studies [3–13].

Color	Pigments
White	calcium carbonate, lead white
Black	black carbon, manganese dioxide
Blue	azurite
Green	malachite
Red	red ochre, vermilion, minium
Yellow	raw sienna, chrome yellow, yellow ochre

Based on the current research, most pigments do not exhibit any visible color alteration after gamma, UV or proton beam irradiation [3,7–12]. Pigments that have been recorded to have undergone significant color changes after irradiation include lead white, calcium carbonate, vermilion, raw sienna, chrome yellow, minium and mars red [6,7,12,13]. The post-irradiation discoloration of lead white and calcium carbonate has been studied intensively. The above two samples could produce dark spots within a few months, regardless of proton beam or gamma radiation [7,9,10,13]. In terms of chromatic change, 26 kGy gamma-irradiated marble dust (calcium carbonate) and flake white (lead white) represented the most significant color shift with ΔE at 6.88 and 3.26, respectively [7]. The effects of irradiation on the gypsum carrier [6] and changes in pigments at different doses and dose rates [4] have also been reported.

At present, there are two main reasons for pigment discoloration caused by radiation. One is the color change caused by irradiation defect and the chemical structure remaining unchanged. From the perspective of irradiation defects, researchers have explained the color changes of the above pigments with the color center theory [7,9,10,13,14]. According to this hypothesis, a paramagnetic color center appears on the surface of the irradiated carbonate pigment, causing color changes. The other is a chemical structural change that causes a change in color. The study of Zafiropulos [15–17] attributed the discoloration of lead white to the change in its chemical structure. After laser irradiation, yellowish flax particles were found in the XRD pattern of lead white powder. In addition, the FT-IR spectrum of γ -irradiated cinnabar [6] also has a slight change. It is speculated that the structural transformation of HgS to β -HgS after irradiation is the cause of color change.

Compared with gamma radiation, electron beam radiation has broad prospects for development due to no radioactive source being needed and higher safety and predictability. The 5 MeV or 10 MeV electron accelerators commonly used in industry are high-energy and heavy, and cannot be moved due to radiation protection, volume, weight, etc., so they can

only be used for the sterilization of movable cultural relics. Murals are immovable cultural relics with complex production techniques, and there are various kinds. The protection methods of mural paintings mainly include environmental control, chemical sterilization, etc. [18,19]. Murals need in situ protection, so conventional electron beam irradiation equipment cannot be used. The development of small intelligent mobile low-energy electron beam irradiation equipment has broadened the application of electron beam irradiation sterilization [20]. According to current reports, it is predicted that small electron beam equipment can be used for in-situ protection of tomb murals. To investigate whether radiation sterilization can realize the protection of mural paintings, it is necessary to investigate the sterilization effect, the influence of the dose of sterilization on the composition and structure of pigments and the influence of the action of pigment bonding materials on the stability of mural paintings, etc. Among them, the bactericidal effect and the influence of mineral pigments are the most direct and effective early evaluation methods. Dahuting Han Tomb is a representative of Chinese tomb murals and Dunhuang Mogao Grottoes are a representative of Chinese cave paintings. The microorganisms in the tomb environment at home and abroad are a complex system. It has been reported that fungi and bacteria coexist and change with seasons [21–23]. As mentioned above, there is little research on the electron beam radiation of mineral pigments at present, and the pigments used in the existing murals in China are all ancient mineral pigments, so it is very important and meaningful to study the radiation effect and its influence mechanism.

In this study, two kinds of microorganisms commonly found in Dahuting Han Tomb, China, were selected as representatives for irradiation sterilization, and the basic sterilization dose was determined. Ancient mineral pigments commonly used in Chinese murals and calcium carbonate in the ground layer were selected as the research objects to verify the sterilization effect of electron beam radiation and the influence of electron beam irradiation on mineral pigments and white pigments commonly used for repairing murals. The potential changes in optical properties and reflectance were quantified using colorimetry and a spectrophotometer. The paramagnetic defects produced by irradiation were characterized using an electron paramagnetic resonance (EPR) spectrum. In addition, X-ray diffraction (XRD), Raman spectra, inductively coupled plasma mass spectrometry (ICP-MS), X-ray fluorescence spectrometry (XRF), X-ray photoelectron spectroscopy (XPS) and X-ray absorption near edge structure (XANES) were used to characterize the structure of the pigments. This work is a preliminary exploration of whether electron beam radiation sterilization can be applied to the in situ protection of immovable cultural relics such as murals. The experimental results can provide basic data for later sterilization research on simulated murals and the nondestructive verification of simulated murals.

2. Materials and Methods

2.1. Test Material and Samples

Penicillium flavogenum (PNC) (fungi) and *Aeromonas hydrophila* (*Aer.h*) (bacteria) were selected as the experimental objects of radiation sterilization (courtesy of the Health and Environment Group, University of Chinese Academy of Sciences). For microbial culture, nutrient agar medium was used for bacteria and potato dextrose agar medium for fungi. The microorganisms were inoculated on an ultraclean table and incubated in a constant-temperature incubator (37 °C for *Aeromonas hydrophila* and 25 °C for *Penicillium flavogenum*).

Among the seven types of ancient Chinese mineral pigments used in this study, malachite ($\text{CuCO}_3 \bullet \text{Cu(OH)}_2$), azurite ($2\text{CuCO}_3 \bullet \text{Cu(OH)}_2$), cinnabar (HgS) and red ochre (Fe_2O_3) were purchased from Lhasa Zahi Rainbow Tibetan Pigment Manufacturing Co., Ltd. A charcoal piece (C) was bought from Marie Painting Materials (Shanghai, China).

For calcium carbonate (CaCO_3), lead white ($2\text{PbCO}_3 \bullet \text{Pb(OH)}_2$) and minium (Pb_3O_4), since standard samples from chemical plants are widely used in current painting restoration, in this study, they were purchased from Baishi Chemical (Tianjin, China), Acme Biochemical (Shanghai, China) and Aladdin Reagent (Shanghai, China) in analytical purity, 99% and 98%, respectively. To further investigate the mechanism of color changes after

irradiation, we also purchased calcium carbonate of analytical purity (99%) manufactured by Aladdin Reagent (Shanghai, China) and lead carbonate basic of analytical purity (99%) produced by Macklin Chemicals (Shanghai, China).

2.2. Electron Beam Irradiation

The electron beam irradiation was performed at room temperature using the Electron LINAC irradiator facility located in Atom-Hitech Co., Ltd. (Beijing, China) with an energy of 10 MeV and a constant dose rate of 5000 Gy/s.

The radiation dose was measured with a GEX B3 film dosimeter. After irradiation, the absorbance at 552 nm was measured with a Yuexi visible spectrophotometer of Shanghai, China, and the absorbed dose was obtained by comparing with the data provided by the GEX.

In the electron beam radiation experiment, sterilization was tested by determining the survival of microorganisms after 5~30 kGy irradiation. Powder pigments were placed in transparent Ziplock bags, and the color was measured after irradiation. One control group and three parallel experimental groups were set up for each experiment group. Seven pigments and calcium carbonate were irradiated at a dose of 10 kGy. Among the eight samples, calcium carbonate (white rock) and lead white (Acmecc) showed more obvious color changes after irradiation. On this basis, experiments were conducted on two calcium carbonates (white stone and Aladdin) and two lead whites (Acmecc and Macklin) at doses of 5~50 kGy in an attempt to study the trend of color change at different doses and the upper limit of pigment color shift under the influence of irradiation.

2.3. Radiation Sterilization Characterization

After irradiation, the microorganisms continued to be cultured in a constant temperature and humidity box for 24~72 h. The growth of microorganisms in the medium was observed and compared with the control group to evaluate the sterilization effect of irradiation.

2.4. Method of Pigment Characterization before and after Radiation

2.4.1. ICP-MS Scan and XRF Analysis

To detect trace elements contained in the samples, two white calcium carbonate-containing pigments and their reference samples were dissolved in 70% HNO₃ and diluted in 2% HNO₃ for ICP-MS SCAN. X-ray fluorescence was performed on the same samples by tableting after mixing with boric acid.

2.4.2. Colorimetry

Color variation was measured with a portable Precision Colorimeter (NR110, Shenzhen ThreeNH Technology Co., Shenzhen, China) in diffuse/8° geometry with a D65 standard light source and 4 mm measuring aperture. For the seven ancient pigments and calcium carbonate, color differences were measured within two hours after irradiation at doses of 0~30 kGy. In addition, the color changes of lead white, calcium carbonate and their reference materials were tracked for 15 days after irradiation at doses ranging from 0 to 30, 40 and 50 kGy. More than four points were taken for each sample during the measurement. Each color parameter was obtained by taking the average of the above four points. CIE 1976 L*a*b* color space and $\Delta E_{00}(1:1:1)$ were used to evaluate color changes. Normally, values of $\Delta E_{76} < 3$ [24,25] or $\Delta E_{00} < 1$ [7] are classified as insignificant.

2.4.3. Spectroscopic Characterization

XRD analyses were performed on a Bruker (D8 Advance) diffractometer with Cu radiation operating at 40 kV and 40 mA. The 2 θ angle was measured at 20–60° for calcium carbonate (Baishi and Acmecc) and 10–70° for lead white (Aladdin and Macklin), both in increments of 0.05. Structural parameters were obtained using JADE software.

Raman spectra were obtained by using a confocal Raman microscope from HORIBA (LabRAM HR Evolution). The system is equipped with a diode laser emitting at 473 nm.

The total acquisition time for each sample was 15 s, with three acquisitions. To avoid sample alteration, the laser power at the sample was set to 75 mW.

UV-vis spectroscopy was performed on Agilent's Cary 5000 (Agilent Technologies, Inc., Santa Clara, CA, USA), measuring wavelengths from 200 to 800 nm. Reflectance spectra of each sample were taken before irradiation, and 1 day, 15 days and 50 days after irradiation. To compare the samples treated with different radiation doses, 0.133 g of calcium carbonate and 0.433 g of lead white were used.

EPR measurements were conducted with an X-band Bruker spectrometer (E500 type) (Bruker Inc., Mannheim, Germany) working at room temperature. Both calcium carbonates were measured in sweep widths 1000 and 105 G and with the following parameters: microwave power 1.002 mW, conversion time 40 ms. Both lead white and hydrocerussite were measured in sweep widths 400 G and with the following parameters: microwave power 1.002 mW, conversion time 40 ms. For EPR measurements, 0.0755 g of calcite-containing samples and 0.2021 g of lead-containing samples were used.

XPS analysis was performed on ESCALAB250 (Thermo Fisher Scientific, Waltham, MA, USA) with a spot size of 500 μm and high-resolution scan energy of 30 eV. The test data was fitted by XPSPEAK software.

The XANES measurements were taken at the Beijing Synchrotron 1W1B Experimental Station. Test standards include $\text{PbCO}_3 \bullet \text{Pb}(\text{OH})_2$, PbCO_3 , $\text{Pb}(\text{OH})_2$, Pb_3O_4 , $\text{Pb}(\text{NO}_3)_2$, PbO , PbSO_4 and pigments of lead white (Acmecc and Macklin) after 30 and 50 kGy irradiation. The pigments and standards used in the tests were collected using transmission mode. The data of the samples were processed with Athena software for energy correction, normalization and background deduction.

3. Results and Discussion

3.1. Electron Beam Radiation Sterilization

The electron beam sterilization experiments of 5, 10, 15, 20, 25 and 30 kGy were carried out for *Aer.h* and *PNC* with a growth cycle of 5 days. The *Aer.h* liquid placed on the medium was also irradiated and sterilized to observe the growth of the liquid before and after irradiation. It can be seen that *Aer.h*, *PNC* and *Aer.h* liquid were effectively killed at the dose of 5~30 kGy.

Figure 1 illustrates the elimination of the two typical strains of tomb bacteria before and after irradiation at 10 kGy, respectively. In the *Aer.h* Petri dish shown in Figure 1, the diameters of a single strain of the unirradiated samples (a) and (b) were 5 mm and 6.5 mm, respectively. In the (c) sample after irradiation, the diameter of a single strain was reduced to 3.5 mm, indicating the effectiveness of electron beam irradiation on *Aer.h* at experimental doses. For *PNC*, the diameters of a single strain in the unirradiated samples (d) and (e) were 11.5 mm and 16 mm, respectively, the colony edges were filamentous and the middle part of the *PNC* strain in sample (e) also showed a mature body of green. However, in the (f) samples irradiated at a suitable temperature and longer preservation time, the colony edges of *PNC* were very regular, and no cyan mature body was formed, which indicated the effectiveness of electron beam at killing *PNC* at a dose of 10 kGy.

In all, after 10 kGy irradiation, these two strains can be effectively removed. Combined with the sterilization effect of radiation on other kinds of microorganisms mentioned in the previous literature [4,6,7], 10 kGy was selected as the effective sterilization dose in this paper for subsequent research.

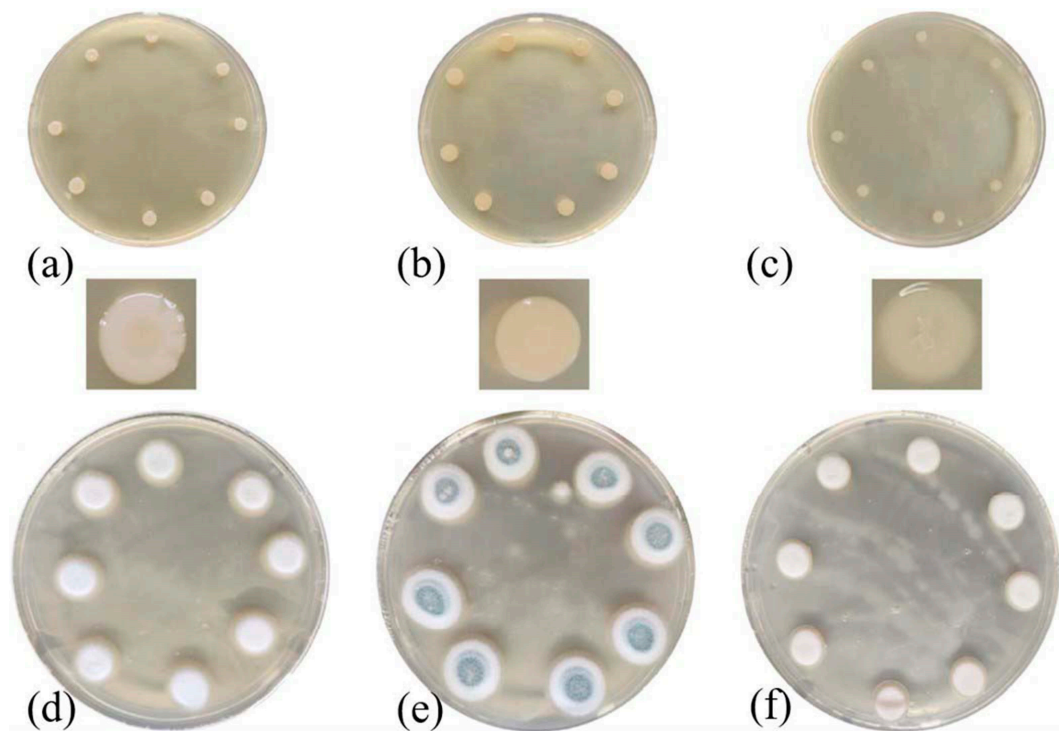


Figure 1. Colony before and after irradiation at 10 kGy. (a–c), respectively, represent the unirradiated *Aer.h* stored at 4 °C, the unirradiated *Aer.h* stored at 37 °C for 36 h and the irradiated *Aer.h* stored at 37 °C for 72 h. (d–f), respectively, refer to the unirradiated PNC preserved at 4 °C, the unirradiated PNC preserved at 25 °C for 24 h and the irradiated PNC preserved at 25 °C for 72 h.

3.2. Electron Beam Radiation Effect of Mineral Pigments

The powder pigments used in this study are all ore pigments commonly used in ancient China, including lead white, minium, charcoal pieces, malachite, azurite, cinnabar and red ochre. Among them, the red pigments cinnabar, red ochre and minium are often used individually or mixed in the Mogao caves [26]. All seven pigments selected were mainly based on the common pigments used in the Mogao caves [26,27], the late Qing Dynasty's Assembly Hall [28] and ancient Tibetan murals [29]. Gypsum or calcium carbonate were used in the ground layer, which also forms calcium carbonate when the gypsum ages naturally. To evaluate the effect of the electron beam, a dosage of 10 kGy, at which most of the fungi could be killed, was chosen as the first irradiation dose for the eight samples [7].

3.2.1. Colorimetric Analysis

Table 2 reflects the color changes of the seven natural mineral pigments and calcium carbonate within 2 h after 10 kGy electron beam irradiation. All the pigments showed $\Delta E_{76} < 3$, $\Delta E_{00} < 1$ within two hours after irradiation except for calcium carbonate (Baishi) and lead white (AcmeC). The color shifts of the above two pigments at 10 kGy exhibit significant color changes, which are similar to the results of the carbonate-based white pigments irradiated using other high-energy rays in all previous articles. After irradiation, the color variations of calcium carbonate and lead white were noticeably higher than the other six pigments, among which the chromatic difference of lead white pigment was significantly higher than calcium carbonate, which ranks as the most affected by irradiation among the seven pigments. Furthermore, a significant decrease in the L value, which represents the luminosity in the color difference parameter, was noticed for both calcium carbonate and lead white after irradiation [7]. In addition, the values of both carbonate-based white pigments showed a slight increase, signifying a slight reddening of the irradiated pigments, a subtle red change that cannot be distinguished by the naked eye, only by using instruments [7]. However, the b values of the above two pigments exhibited

opposite and more marked changes. Measurements of the *b* values of calcium carbonate (Baishi) exhibit a decrease, while lead white (Acmecc) shows an increase. The decreasing *b* value of calcium carbonate from Baishi illustrates a blue-biased color change in response to irradiation [6], whereas the increase in the *b* value of lead white from Acmecc indicates a yellowish color change after irradiation [7,13].

Table 2. Color changes of the seven natural mineral pigments and calcium carbonate within 2 h after 10 kGy E-beam irradiation.

Samples	Dose	L	a	b	ΔE_{76}	ΔE_{00}
Calcium carbonate (Baishi)	before	97.661	−0.738	0.641		
	10 kGy	93.904	0.48	−1.046	4.29	3.29
Lead white(Acmecc)	before	97.574	−1.516	1.487		
	10 kGy	92.121	−0.259	5.773	7.05	5.31
Minium	before	67.606	42.777	40.65		
	10 kGy	67.78	40.742	39.634	2.28	0.75
Charcoal piece	before	44.109	−0.013	−0.334		
	10 kGy	44.703	0.019	−0.223	0.61	0.57
Malachite	before	74.285	−10.494	3.686		
	10 kGy	73.595	−10.508	3.925	0.73	0.54
Azurite	before	68.337	−6.296	−7.104		
	10 kGy	67.969	−6.537	−6.031	1.16	0.95
Cinnabar	before	58.782	30.919	22.213		
	10 kGy	58.927	30.999	22.96	0.77	0.45
Red ochre	before	54.153	17.895	11.661		
	10 kGy	55.083	17.849	11.507	0.94	0.89

In order to explore the cause of the discoloration of calcium carbonate (Baishi) and lead white (Acmecc) at 10 kGy, calcium carbonate from Aladdin Reagents and lead white from Macklin were purchased for comparative analysis. In the subsequent irradiation experiments at 5~50 kGy, four white samples were analyzed.

Figure 2 shows the variation in *L*, *a* and *b* for two calcium carbonate (Baishi and Aladdin) and two lead white samples (Acmecc and Macklin) after irradiation with an electron beam at doses from 0 to 50 kGy. As can be seen from the four samples in Figure 1, the *L* values have exhibited the most pronounced decrease, which represents the decrease in the brightness of the samples after electron beam treatment. The *L* values of the two calcium carbonate samples, along with the lead white from Acmecc, turned at 30 kGy. Before 30 kGy, the *L* values of the above three samples kept decreasing with increasing doses. At doses of 30~50 kGy, despite the dosage still increasing, the *L* values of the samples stopped decreasing. In addition, calcium carbonates from Baishi and Aladdin both show a decrease in “*b*” and increase in “*a*” after irradiation; the *a* and *b* values of both lead white samples increased.

To evaluate the total variation in all four samples, the color difference values of the samples at 5~50 kGy were calculated. Table 3 show that the difference for calcium carbonate from Aladdin was higher than that of Baishi’s calcium carbonate at the same dose. The color difference between two calcium carbonate-containing samples appeared to saturate after 30 kGy. Subsequent increases in dose did not bring noticeable changes in the chromatic of the samples. For lead white from Acmecc and Macklin, before 10 kGy, the color difference of lead white (Acmecc) was higher than hydrocerussite (Macklin). After 10 kGy, the color difference of the two samples was uniform. At 30~50 kGy, the color difference of lead white from Acmecc also showed a saturation similar to the two calcium carbonate samples. In contrast, the color variation of lead white from Macklin kept increasing with the irradiation dose.

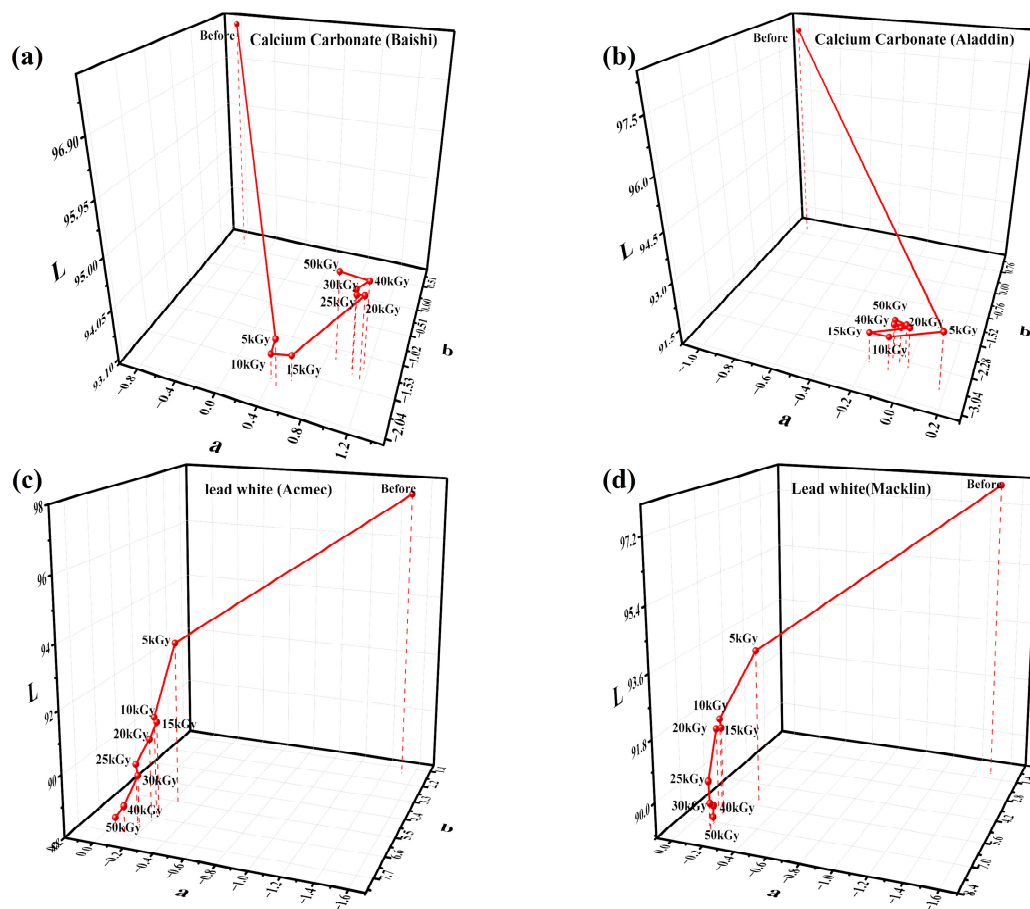


Figure 2. Variation in L, a and b values of calcium carbonate from (a) Baishi and (b) Aladdin and lead white from (c) Acmeec and (d) Macklin under different irradiation doses.

Table 3. Color change of calcium carbonate and lead white at different doses.

Dose (kGy)	ΔE_{00}			
	Calcium Carbonate (Baishi)	Calcium Carbonate (Aladdin)	Lead White (Acmeec)	Lead White (Macklin)
5	3.45	4.38	4.41	3.72
10	3.29	4.6	5.31	3.81
15	4	4.83	5.68	5.74
20	3.99	4.95	6	5.73
25	4.4	5.01	6.22	6.85
30	4.47	5.35	7.84	7.27
40	4.18	5.32	8.17	7.49
50	4.31	5.29	8.09	8.06

3.2.2. Study on the Mechanism of Radiation-Induced Discoloration

Figure 3 shows the UV-visible diffuse reflectance spectra of four carbonate-containing samples on the first day after irradiation, with an electron beam energy of 10 MeV, a dose of 0~50 kGy and a dose rate of 5000 Gy/s. Figure 3 reveals that the stratification of the diffuse reflectance spectra of the two lead white samples becomes more obvious after different doses of irradiation, while the reflectance of calcium carbonate from Baishi and Aladdin differs slightly between different doses. This shows a higher effect of irradiation dose on the reflectance of the two lead white samples compared with the two calcium carbonate-containing samples. With the higher irradiation dose, the reflectance of lead

white (Acme and Macklin) decreases sharply in the visible band. The performance of the reflectance of the four samples in the UV-vis diffuse reflectance spectra is consistent with the results of the color difference, with the largest color difference value of 1 between different doses for the two calcium carbonate samples and 4 for the two lead white samples. The similar performances of all four samples in the UV-vis diffuse reflectance spectra and chromatic variation collectively indicate that the color changes of the lead white samples are more pronounced with different doses.

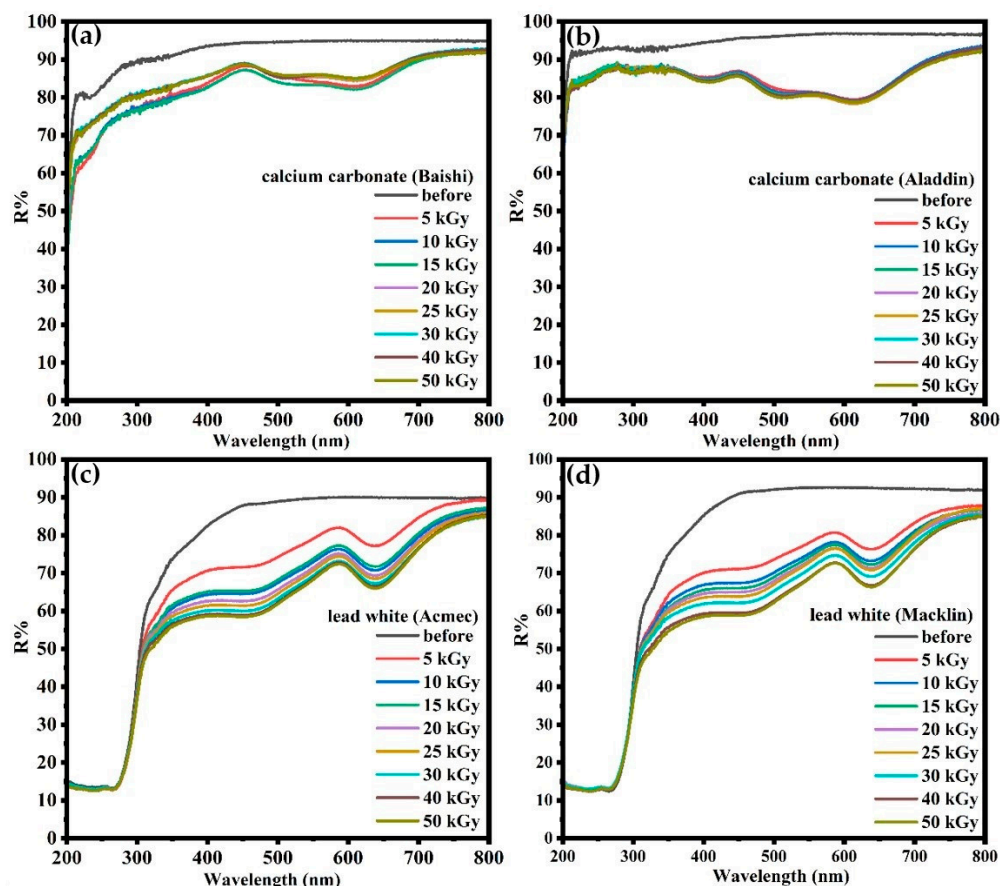


Figure 3. UV-Vis diffuse reflectance spectra of the calcium carbonate from (a) Baishi and (b) Aladdin and lead white from (c) Acme and (d) Macklin within 1 d after 0~50 kGy irradiation.

In the UV-vis diffuse reflectance spectra of lead white from Acme and Macklin, a distinct signal peak can be observed in the yellow region of 570~600 nm in Figure 3. This means a significant yellowing of the samples after irradiation, which corresponds to an increase in the *b* value of the samples during the color difference measurement [30]. Moreover, although no peaks were formed at 750 nm after irradiation, the reflectance of the two lead white samples at 750 nm did not show the same decay as the rest of the visible band. Such an observation further confirms a slight increase in *a* value and a minor reddening of the two irradiated lead-containing samples [30].

For calcium carbonate from Baishi and Aladdin, the new signal peak at 400~480 nm after irradiation shows the blueish color shift of the sample, which also matches the decrease in *b* value [30]. In addition, the unique performance of the two lead-containing samples at 750 nm also appears for the two samples containing calcium carbonate, which corresponds to a slight reddening of the color and an elevated *a* value [30].

From the diffuse reflectance spectra and chromatic aberration measurements, both calcium carbonate samples as well as lead white from Acme exhibit saturation levels at doses of 30 kGy. For lead white from Macklin, doses of 50 kGy did not saturate its color changes or the signal intensity of the diffuse reflectance spectrum. A similar saturation phenomenon was also present for the marble dust (calcium carbonate), flake white historical (lead white)

and terra alba after gamma irradiation, but the dose became 15 kGy [2]. Meanwhile, not all white materials containing carbonate show chromatic aberration or saturation of the diffuse reflectance spectrum after high-dose irradiation. In the study conducted by Marušić et al., gamma-irradiated nacres did not exhibit any signs of saturation, even with a dose of 56 kGy [30]. In light of this, it can be assumed that color saturation occurs with increasing doses of calcium carbonate and lead white, but the doses for saturation vary between different materials and irradiation sources.

Based on the manifestation of chromatic variations in the irradiated samples, the following experiments were conducted by using samples and a dose of 30 kGy. A comparison of the UV-vis diffuse reflectance spectra of four samples irradiated at 30 kGy and kept at room temperature for different times is shown in Figure 4. It highlights that the reflectance of the irradiated samples, which had been left at room temperature for a while, regained its reflectance in the visible band. The reflectance of the two calcium carbonate samples showed only a slight increase before and after 15 days, while the reflection of two lead white samples showed a relatively obvious rebound after 15 days at room temperature. The different performance in terms of reflectance accounted for the worse stability of chromatic variation after irradiation for the two lead-containing samples.

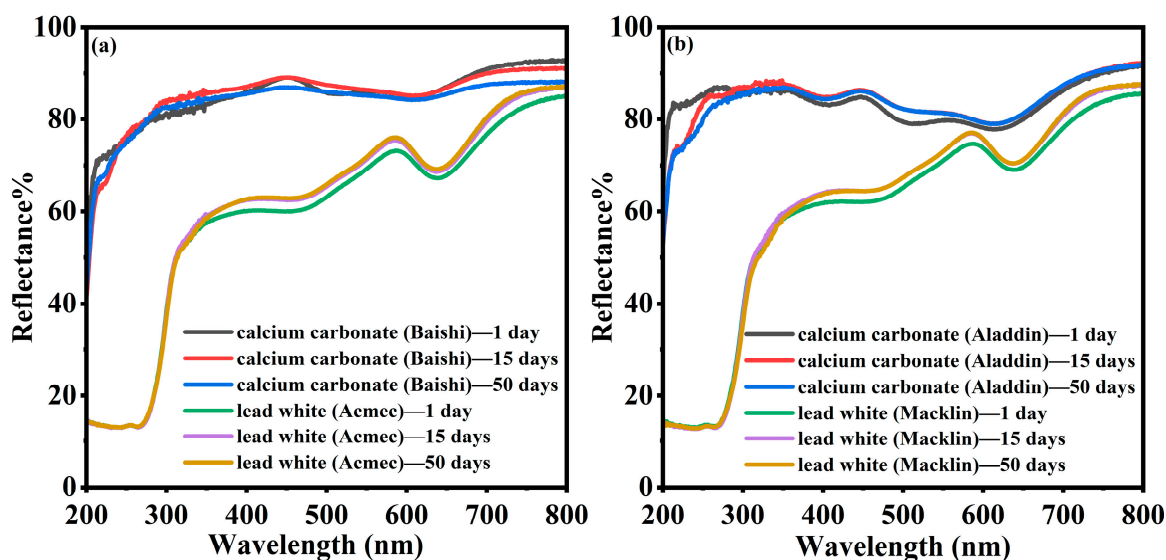


Figure 4. Comparison of diffuse reflection spectra of 30 kGy-irradiated calcium carbonate [(a) Baishi and (b) Aladdin] and lead white [(a) Acmec and (b) Macklin] samples stored for 1~50 days.

Figure 5 shows the changes in the calcium carbonate (Baishi) and lead white (Acmec) after 30 kGy irradiation. There was optical variation, as mentioned above, with bluish and yellowish changes emerging on calcium carbonate and lead white, respectively. Further, there was a noticeable degradation in the brightness of the above two pigments after irradiation.

Figure 6 exhibits the stability of color changes for the four samples irradiated at 30 kGy. For the two calcium carbonate samples, no significant changes could be detected between 1 day and 150 days. However, values at 150 d for the two lead white samples decreased by more than 50% compared to 1 day. Based on the findings above, better time stability of color changes of the two calcium carbonate-containing samples was obtained. Owing to the worse stability, the color difference of the two lead-containing samples began to be lower than that of the two calcium carbonates after 60 days. Overall, up to four months at room temperature did not make the color difference of all four samples indistinguishable, as chromatic variation values of these samples were still higher than 1 after 150 days, and the color difference value stabilized after 90 days. Investigations into the stability of color changes of such carbonate-based white pigments have also been discussed in other papers. According to Negut et al. [7], the stability of color changes of marble dust irradiated by

gamma rays at 26 kGy remained good, with no recovery of its initial color despite a year of storage at room temperature. Meanwhile, the color shifts of flake white historical dropped to 1 within 90 days. According to the same decreasing trend of the color of two lead white samples in our experiments, the value of chromatic variation will drop to less than 1 with enough storage time provided.

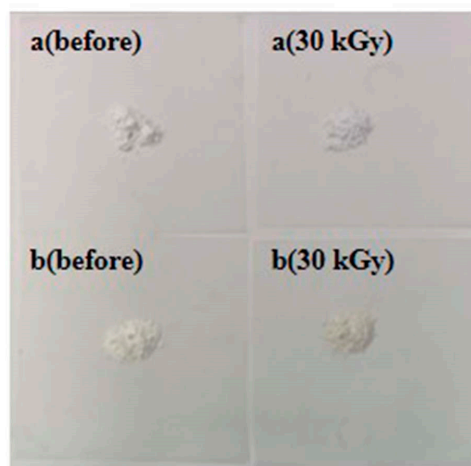


Figure 5. Optical variations of (a) calcium carbonate (Baishi) and (b) lead white (Acmecc) under E-beam irradiation.

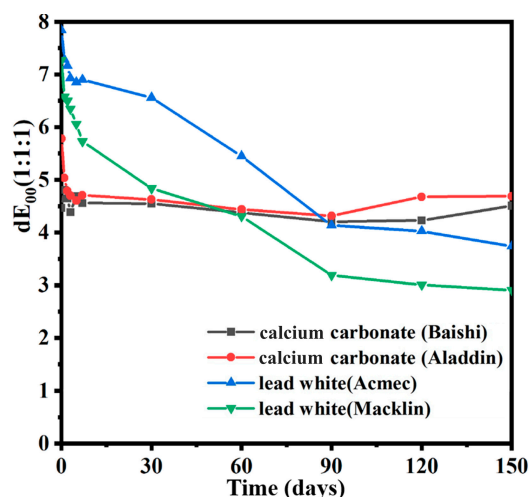


Figure 6. Time variation in color difference of calcium carbonate and lead white samples irradiated using an electron beam.

Since the irradiation treatment was not supposed to have any impact on the elemental content of the samples, a qualitative analysis of the elements within the two white carbonate-based samples was performed. Slightly different results were obtained, with different detection limits with varying instruments. Table 4 shows the elemental composition of lead white (Acmecc) and calcium carbonate (Baishi). More impurities were detected within the calcium carbonate from Baishi, such as the symbolic element Sr in natural minerals, and the typical impurities Mn and Mg in calcite or dolomite. [31]. In contrast, no elements were detected in the lead white from Acmecc except for Pb.

Table 4. Elemental composition of calcium carbonate from Baishi and lead white from Acmecc.

Pigments	XRF	ICP-MS
calcium carbonate (Baishi)	Ca, Sr	Ca, Mg, Sr, Mn
lead white (Acmecc)	Pb	Pb

In order to explain the mechanism of discoloration, selected characterization experiments were conducted on samples before and after 30 kGy irradiation. XRD spectra of the original sample and sample with 30 kGy irradiation were obtained, and are shown in Figure 7a~d. The blue lines are the diffraction peaks of the corresponding reference materials in Jade, the XRD data analysis software. As can be seen from the figure, it is consistent with the actual test peak of the sample. Compared with the original sample, no substantial modifications to the crystal phase were observed in the samples irradiated at 30 kGy. This means that no phase destruction occurred during irradiation, which contradicts the theory of variation in chemical structure leading to color modification [15]. However, the reduction intensity of the peaks observed in the samples indicates a decrease in the crystallinity after irradiation [32].

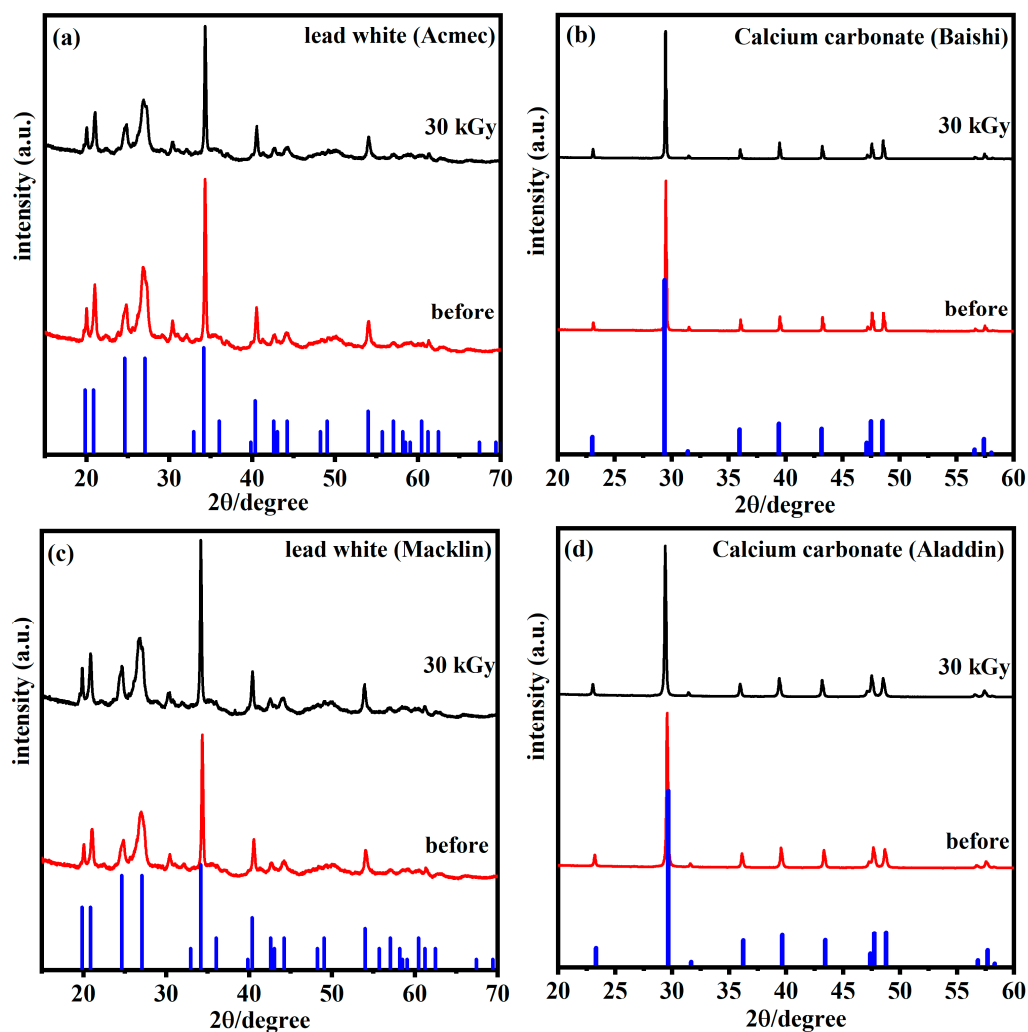


Figure 7. XRD spectra of lead white from (a) Acmecc and (c) Macklin and calcium carbonate from (b) Baishi and (d) Aladdin before and after irradiation.

Figure 8 gives the Raman spectra of irradiated and unirradiated samples. Three peaks with signals at 281, 711 and 1086 cm^{-1} represent the stretching vibration of the C-O within the calcium carbonate from both Baishi and Aladdin, while a signal at 1049 cm^{-1} of the two lead white samples represents the stretching vibration of the carbonate ion [32,33]. The unchanged positions of Raman peaks equally indicate the stable structure of the four samples after irradiation. Moreover, decreased peak intensities suggest that the electron redistribution on the strength of the photon-phonon coupling was influenced [34].

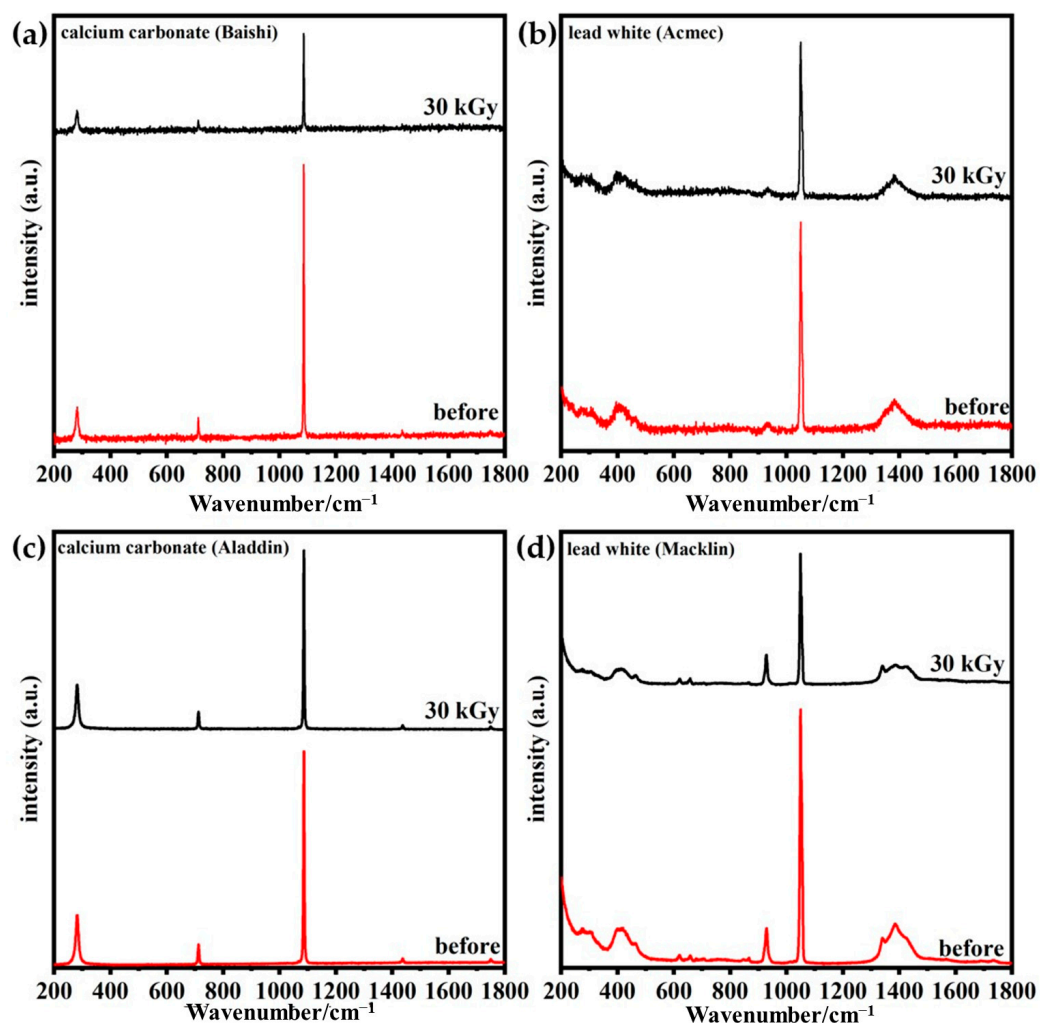


Figure 8. Raman spectra of calcium carbonate from (a) Baishi and (c) Aladdin and lead white from (b) Acmec and (d) Macklin samples before and after irradiation.

The XPS spectra of the O1s of the two lead white samples before and after irradiation are shown in Figure 9. The XPS map of lead white is divided into three forms of Pb, and the red line is the result of fitting three speculated forms. By comparing with the original map, it is reasonable to determine that PbCO_3 , Pb(OH)_2 and PbO are the three substances with peak. The XPS spectra of the two lead white samples are consistent with the characteristics of basic lead carbonate. The signal peaks of the samples at 531.3 eV and 532.6 eV stand for PbCO_3 and Pb(OH)_2 , respectively [35]. Furthermore, a peak at 529.6 eV representing the PbO signal was also found in the two lead white pigments. In previous studies, the signal at 529.6 eV was generally not observed in the pre-irradiated lead white, but was more pronounced in the post-irradiated ones [35,36]. Since no alteration in the intensity of the O1s signal of the lead white samples was detected after irradiation, it was concluded that no morphological changes emerge in the sample during irradiation.

Pb_{III} -edge XANES spectra (normalized) of seven reference materials and four lead white pigments (after irradiation) are shown in Figure 10. The XANES peak of the four lead white pigments is consistent with those of the reference materials of basic lead carbonate without shifts. The EXANES spectra differed between the different reference samples, where the apparent right shift of Pb_3O_4 is due to the stronger nuclear attraction of the higher oxidation state Pb [37]. The EXANES peaks of reference substances other than Pb_3O_4 are also displaced compared to the alkali lead carbonate, which can be explained by the interactions between Pb and different ligand types [37]. Since no shift of the XANES peaks occurred, the chemical structure of lead white is not thought to be altered after irradiation.

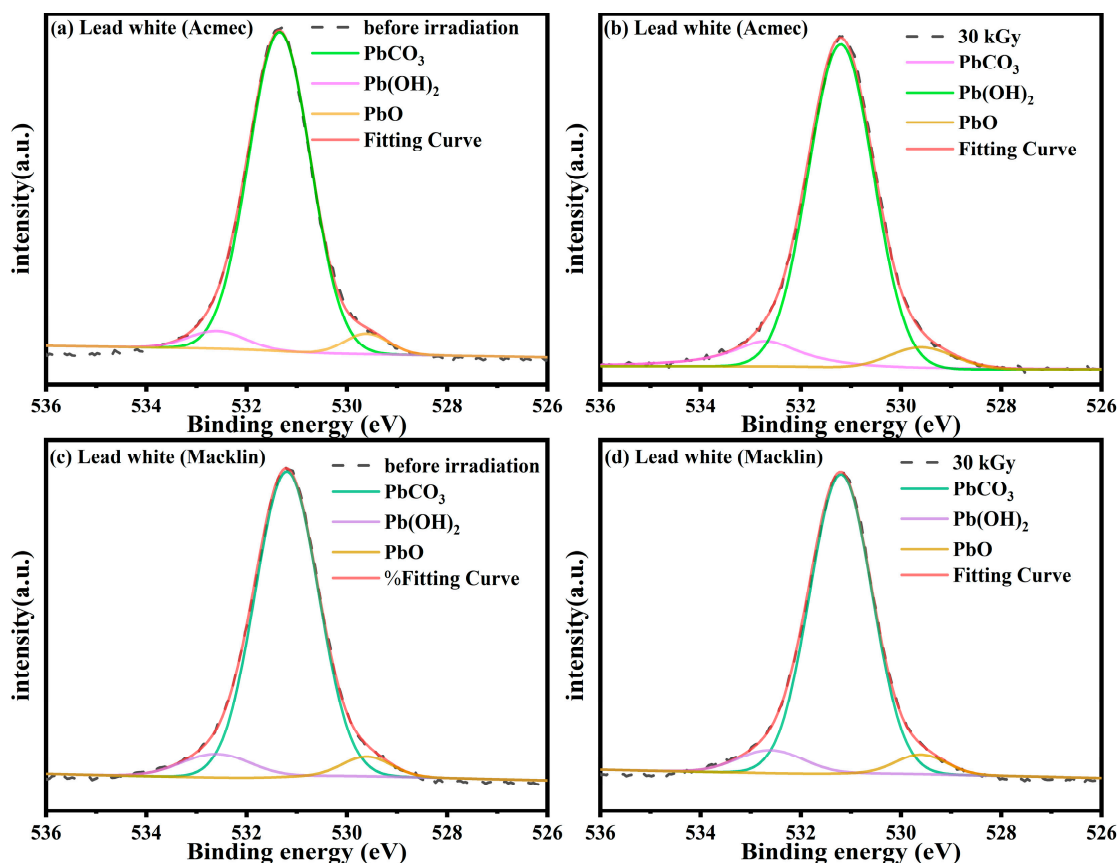


Figure 9. Comparison of XPS spectra of O 1s in lead white before and after irradiation. (a) Acmec, 0 kGy; (b) Acmec, 30 kGy; (c) Macklin, 0 kGy and (d) Macklin, 30 kGy.

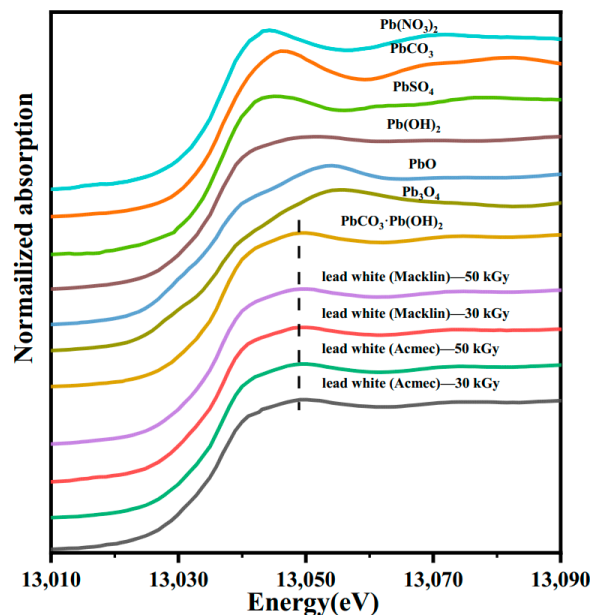


Figure 10. XANES spectra of reference materials and lead white pigments at Pb L_{III} edge.

All EPR spectra of the four color-changing samples were obtained at room temperature one day after irradiation. In Figure 11, a six-line spectrum is noted on both two calcium carbonate samples with the same position but different intensities. Such a six-line structure, generated by the hyperfine interaction between the nuclear spin and the electron spin of $^{25}\text{Mn}^{2+}$, indicates the presence of Mn within the measured samples [7,38]. Consistent

with the above characterization results, the common impurity Mn is found within the EPR spectrum of calcium carbonate from Baishi and Aladdin.

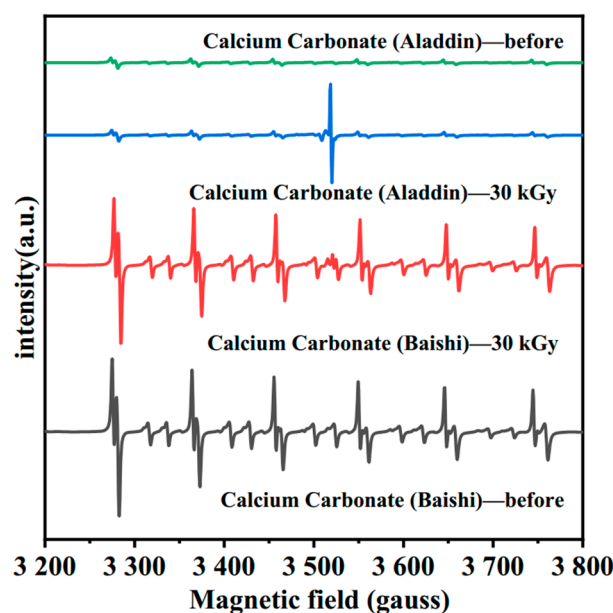


Figure 11. EPR spectra of calcium carbonate from Baishi and Aladdin before and after 30 kGy E-beam irradiation.

The relatively strong six-line spectrum intensity and broader resonance lines in calcium carbonate from Baishi indicate its high Mn content [38]. Additionally, similar to the peaks created by gamma irradiation, signals between the third and fourth lines of the Mn^{2+} hyperfine structure lines indicate the production of color centers or other paramagnetic defects in the two calcium carbonate-containing samples after E-beam irradiation [7,38].

As shown in Figure 12, signals of two calcium carbonate-containing samples were finely scanned between the third and fourth lines of Mn^{2+} . According to Figure 12a, distinct isotropic paramagnetic defects with $g = 1.9998$ appear in the irradiated calcium carbonate (Aladdin). Compared with previous research, such an isotropic defect at $g = 1.9998$ may be formed by an electron trapped in a CO_2^- vacancy during the grinding of calcium carbonate, which is also denoted as an F^+ center [38]. Meanwhile, two groups of anisotropic radicals also appeared on the irradiated calcite, one identified as CO_2^- orthorhombic with $g_1 = 2.0033$, $g_2 = 2.0017$ and $g_3 = 1.9974$, while the other group was classified as CO_3^- orthorhombic with $g_1 = 2.0217$, $g_2 = 2.0071$ and $g_3 = 2.0057$. Both of the above paramagnetic defects have been found in calcium carbonate which irradiated with gamma [39], UV [40] and X-rays [38]. In Figure 12b, a similar approach was also analyzed for calcium carbonate from Baishi treated at 30 kGy. It is clear that the isotropic defect at $g = 1.9998$ still appears, and although the intensity of the signal here is not as strong as that of its reference sample, it still belongs to the same color center generated during grinding.

However, we cannot make a definite diagnosis of the peak at $g = 2.0028$ due to the high interference of Mn impurities. According to previous studies, this peak might correspond to some carbonate defects arising after irradiation [38–40]. Since electrons cannot maintain such a trapped state, the intensity of the color centers appearing above is supposed to decrease with time [7]. Such similar time stability of color difference and UV-vis intensity reinforces the correlation between the color center and color changes of pigments after E-beam irradiation.

Despite the absence of Mn^{2+} impurities in the sample, peaks around $g = 2$ were still found in the white lead (Acme) after E-beam irradiation, as seen in Figure 13. The paramagnetic defects of the irradiated lead white from Macklin were consistent with the lead white from Acme, with three overlapping peaks. Limited by the current detection conditions, the separation and characterization of the above three peaks seem infeasible.

Therefore, combined with previous studies, the value of g -factor approaching 2 indicates that unpaired electrons are captured after electron beam irradiation. This electron–electron defect state causes a change in the color of the two types of lead.

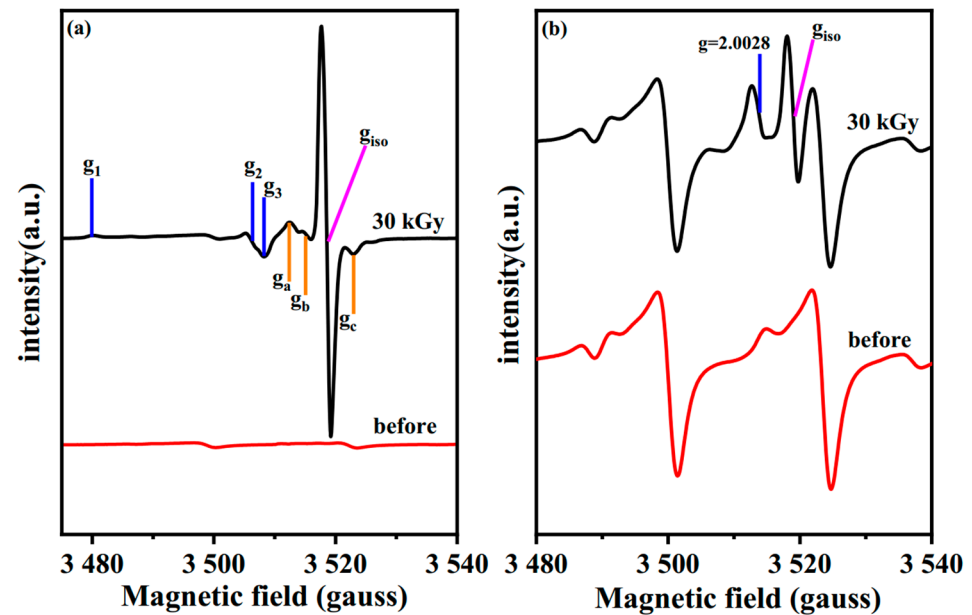


Figure 12. EPR spectra of calcium carbonate from (a) Aladdin and (b) Baishi between the third and fourth lines of Mn^{2+} .

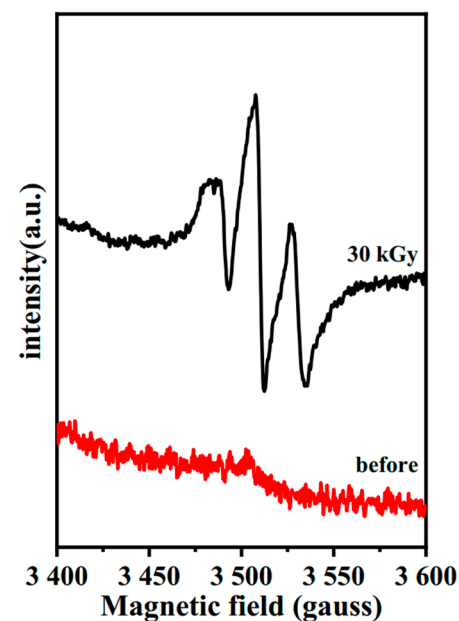


Figure 13. EPR spectra of lead white from Acme.

4. Conclusions

Herein, *PNC* and *Aer.h*, which are widely present in the Han tomb of Dahuting, China, were taken as typical microorganisms, and it was indicated that 10 kGy electron beam irradiation could effectively kill bacteria with a culture cycle of 5 days in a medium, which confirmed the effectiveness of irradiation sterilization. The effect of electron beam radiation on seven powder mineral pigments and calcium carbonate used in mural paintings under an effective sterilization dose was studied in detail. Minium, charcoal pieces, malachite, azurite, cinnabar and red ochre showed no obvious color change after 10 kGy irradiation. The color difference of calcium carbonate and lead white before and after irradiation

increased with the increase in dose and gradually saturated after 30 kGy. Compared with gamma, proton and X-ray radiation, the time stability of the color difference of calcium carbonate and lead white samples after electron beam treatment is better. The mechanism of the radiative discoloration of white pigment caused by an electron beam was studied in this paper. XRD, Raman, XPS and EXANS spectra show that the structure of the powder samples has no change after irradiation. The EPR test confirms the formation of free radicals in the sample after electron beam radiation. According to the above results, the color changes of the calcium carbonate and lead white samples are most reasonably attributed to color center changes. The color center is formed by the combination of unpaired electrons and defects in the process of electron beam irradiation. After forming the new color center, the light absorption curves of the four samples also changed, which was consistent with the previous data. Moreover, such reversible changes take a long time to be reversed, returning the sample to the original state.

The results show that electron beam irradiation has certain application potential in the sterilization and protection of frescoes. The radiation treatment can greatly reduce the microbial contamination at the right dose and has little effect on the color mineral pigments. Electron beam radiation sterilization technology has no residue, has little impact on the environment and does not cause secondary pollution. In a later stage, the sterilization effect will be verified by the irradiation of more tomb microorganisms and mixed microbial samples with electron beam radiation. Irradiation studies will also be carried out on simulated mural blocks made with reference to actual mural techniques to investigate factors such as temperature and humidity and study the changes of pigments under mural conditions. Obtaining more experimental data can guide the application of small mobile intelligent electron beam irradiation equipment in the protection of immovable cultural relics. The method of restoring the original color center of white pigment was also discussed. Further research can promote the application of this method in the protection of related cultural relics.

Author Contributions: M.L. was responsible for the design of the whole experiment and the writing of this paper. P.B. was responsible for specific pigment irradiation experiments and the analysis of various spectral characterization results. Y.S. was responsible for irradiation sterilization experiments. Z.L. was responsible for the detection and analysis of electron paramagnetic resonance. L.M. and D.X. were responsible for checking and revising the article and provided financial support. All authors have read and agreed to the published version of the manuscript.

Funding: This research was funded by the National key research and development program of China (2019YFC1520700) and the Science and technology planning project of Sichuan province (2022YFSY0032).

Data Availability Statement: Not applicable.

Acknowledgments: We would like to thank the University of Chinese Academy of Sciences for their support (microorganisms provided by the health and environment group).

Conflicts of Interest: The authors declare no conflict of interest.

References

1. Ciferri, O. Microbial degradation of paintings. *Appl. Environ. Microbiol.* **1999**, *65*, 879–885. [[CrossRef](#)] [[PubMed](#)]
2. Cappitelli, F.; Cattò, C.; Villa, F. The control of cultural heritage microbial deterioration. *Microorganisms* **2020**, *8*, 1542. [[CrossRef](#)]
3. Manea, M.M.; Moise, I.V.; Virgolici, M.; Negut, C.D.; Barbu, O.-H.; Cutrubinis, M.; Fugaru, V.; Stanculescu, I.R.; Ponta, C.C. Spectroscopic evaluation of painted layer structural changes induced by gamma radiation in experimental models. *Radiat. Phys. Chem.* **2012**, *81*, 160–167. [[CrossRef](#)]
4. Sakr, A.A.; Ghaly, M.F.; Edwards, H.G.M.; Elbasha, Y.H. Gamma-radiation combined with tricycloazole to protect tempera paintings in ancient Egyptian tombs (Nile Delta, Lower Egypt). *J. Radioanal. Nucl. Chem.* **2019**, *321*, 263–276. [[CrossRef](#)]
5. Manea, M.M.; Negut, C.; Stanculescu, I.R.; Ponta, C. Irradiation effects on canvas oil painting: Spectroscopic observations. *Radiat. Phys. Chem.* **2012**, *81*, 1595–1599. [[CrossRef](#)]
6. Cortella, L.; Albino, C.; Tran, Q.-K.; Froment, K. 50 years of French experience in using gamma rays as a tool for cultural heritage remedial conservation. *Radiat. Phys. Chem.* **2020**, *171*, 108726. [[CrossRef](#)]

7. Negut, C.D.; Bercu, V.; Dului, O.G. Defects induced by gamma irradiation in historical pigments. *J. Cult. Herit.* **2012**, *13*, 397–403. [[CrossRef](#)]
8. Zheng, L.; Wang, Z.; Shen, S.; Xia, Y.; Li, Y.; Hu, D. Blurring of ancient wall paintings caused by binder decay in the pigment layer. *Sci. Rep.* **2020**, *10*, 21075. [[CrossRef](#)] [[PubMed](#)]
9. Gourier, D.; Binet, L.; Gonzalez, V.; Vezin, H.; Touati, N.; Calligaro, T. Effect of analytical proton beam irradiation on lead-white pigments, characterized by EPR spectroscopy. *Nucl. Instrum. Methods Phys. Res. Sect. B Beam Interact. Mater. At.* **2018**, *415*, 64–71. [[CrossRef](#)]
10. Absil, J.; Garnir, H.-P.; Strivay, D.; Oger, C.; Weber, G. Study of color centers induced by PIXE irradiation. *Nucl. Instrum. Methods Phys. Res. Sect. B Beam Interact. Mater. At.* **2002**, *198*, 90–97. [[CrossRef](#)]
11. Pfendler, S.; Einhorn, O.; Karimi, B.; Bousta, F.; Cailhol, D.; Alaoui-Sosse, L.; Alaoui-Sosse, B.; Aleya, L. UV-C as an efficient means to combat biofilm formation in show caves: Evidence from the La Glacière Cave (France) and laboratory experiments. *Environ. Sci. Pollut. Res.* **2017**, *24*, 24611–24623. [[CrossRef](#)] [[PubMed](#)]
12. Negut, D.C.; Ponta, C.C.; Georgescu, R.M.; Moise, I.V.; Niculescu, G.; Lupu, A.I.M. Effects of gamma irradiation on the colour of pigments / /O₃A: Optics for Arts, Architecture, and Archaeology. In Proceedings of the International Society for Optics and Photonics, Munich, Germany, 17–21 June 2007; Volume 6618, p. 66180R.
13. Calligaro, T.; Gonzalez, V.; Pichon, L. PIXE analysis of historical paintings: Is the gain worth the risk? *Nucl. Instrum. Methods Phys. Res. Sect. B Beam Interact. Mater. At.* **2015**, *363*, 135–143. [[CrossRef](#)]
14. Enguita, O.; Calderón, T.; Fernández-Jiménez, M.; Beneitez, P.; Millan, A.; García, G. Damage induced by proton irradiation in carbonate based natural painting pigments. *Nucl. Instrum. Methods Phys. Res. Sect. B Beam Interact. Mater. At.* **2004**, *219*, 53–56. [[CrossRef](#)]
15. Zafiropoulos, V.; Stratoudaki, T.; Manousaki, A.; Melesanaki, K.; Oriol, G. Discoloration of pigments induced by laser irradiation. *Surf. Eng.* **2001**, *17*, 249–253. [[CrossRef](#)]
16. Vagnini, M.; Vivani, R.; Sgamellotti, A.; Miliiani, C. Blackening of lead white: Study of model paintings. *J. Raman Spectrosc.* **2020**, *51*, 1118–1126. [[CrossRef](#)]
17. Gliozzo, E.; Ionescu, C. Pigments—Lead-based whites, reds, yellows and oranges and their alteration phases. *Archaeol. Anthropol. Sci.* **2022**, *14*, 17. [[CrossRef](#)]
18. Paolo, M.; Laura, M.; Paul, P. *Conservation of Wall Paintings*; Butterworths: London, UK, 1984.
19. Cesare, B. *Theory of Restoration*; Istituto Centrale per il Restauro: Roma, Italy, 2005.
20. Xu, D.; Shi, R.; Ma, L.; Ruan, Y.; Luo, M.; Dai, M.; Shao, Y.; Zhuo, L.; Yang, X. Intelligently Controlled Mobile Electron Beam Irradiation Device. Chinese Patent ZL 202022634267.X, 11 February 2022.
21. Liu, Z.; Zhu, H.; Wu, M.; Li, Y.; Cao, H.; Rong, R. Seasonal dynamics of airborne culturable fungi and its year-round diversity monitoring in Dahuting Han Dynasty Tomb of China. *Sci. Total Environ.* **2022**, *838*, 155990. [[CrossRef](#)]
22. Liu, W.; Zhou, X.; Jin, T.; Li, Y.; Wu, B.; Yu, D.; Yu, Z.; Su, B.; Chen, R.; Feng, Y.; et al. Multikingdom interactions govern the microbiome in subterranean cultural heritage sites. *Proc. Natl. Acad. Sci. USA* **2022**, *119*, e2121141119. [[CrossRef](#)]
23. Zucconi, L.; Canini, F.; Isola, D.; Caneva, G. Fungi affecting wall paintings of historical value: A worldwide meta-analysis of their detected diversity. *Appl. Sci.* **2022**, *12*, 2988. [[CrossRef](#)]
24. Cardell, C.; Herrera, A.; Guerra, I.; Navas, N.; Simón, L.R.; Elert, K. Pigment-size effect on the physico-chemical behavior of azurite-tempera dosimeters upon natural and accelerated photo aging. *Dye. Pigment.* **2017**, *141*, 53–65. [[CrossRef](#)]
25. Elert, K.; Cardell, C. Weathering behavior of cinnabar-based tempera paints upon natural and accelerated aging. *Spectrochim. Acta Part A Mol. Biomol. Spectrosc.* **2019**, *216*, 236–248. [[CrossRef](#)]
26. Liang, J.; Wan, X. Prototype of a pigments color chart for the digital conservation of ancient murals. *J. Electron. Imaging* **2017**, *26*, 023013. [[CrossRef](#)]
27. Zhang, Y.; Wang, J.; Liu, H.; Wang, X.; Zhang, S. Integrated analysis of pigments on murals and sculptures in Mogao Grottoes. *Anal. Lett.* **2015**, *48*, 2400–2413. [[CrossRef](#)]
28. Hu, K.; Bai, C.; Ma, L.; Bai, K.; Liu, D.; Fan, B. A study on the painting techniques and materials of the murals in the Five Northern Provinces' Assembly Hall, Ziyang, China. *Herit. Sci.* **2013**, *1*, 18. [[CrossRef](#)]
29. Wu, M.; Zou, X.; Zhang, B.; Zhao, F.; Xie, Z. Immunological methods for the detection of binders in ancient Tibetan murals. *Microsc. Microanal.* **2019**, *25*, 822–829. [[CrossRef](#)]
30. Marušić, K.; Pucić, I.; Desnica, V. Ornaments in radiation treatment of cultural heritage: Color and UV-vis spectral changes in irradiated naces. *Radiat. Phys. Chem.* **2016**, *124*, 62–67. [[CrossRef](#)]
31. Dului, O.G.; Bercu, V.; Negut, D.C. Mn²⁺ EPR spectroscopy for the provenance study of natural carbonates. *Exp. Methods Phys. Sci.* **2019**, *50*, 1–19.
32. Qi, Q.; Wang, J.; Xiang, M.; Zhang, Y.; Gu, S.; Luo, G.-N. Mechanism of vacuum-annealing defects and its effect on release behavior of hydrogen isotopes in Li₂TiO₃. *Int. J. Hydrog. Energy* **2018**, *43*, 12295–12301. [[CrossRef](#)]
33. Frausto-Reyes, C.; Ortiz-Morales, M.; Bujdud-Pérez, J.; Magaña-Cota, G.; Mejía-Falcón, R. Raman spectroscopy for the identification of pigments and color measurement in Dugès watercolors. *Spectrochim. Acta Part A Mol. Biomol. Spectrosc.* **2009**, *74*, 1275–1279. [[CrossRef](#)]
34. Junior, H.J.L.; Duarte, C.A.; Pinto, M.W.S.; Foryta, D.W.; Titon, B.G.; Vasconcellos, E.M.G. Influence of gamma ray irradiation on the optical properties of calcite and dolomite. *Appl. Spectrosc.* **2020**, *74*, 507–514. [[CrossRef](#)]

35. Bruder, R.; L'Hermite, D.; Semerok, A.; Salmon, L.; Detalle, V. Near-crater discoloration of white lead in wall paintings during laser induced breakdown spectroscopy analysis. *Spectrochim. Acta Part B At. Spectrosc.* **2007**, *62*, 1590–1596. [[CrossRef](#)]
36. Beck, L.; Gutiérrez, P.; Miserque, F.; Thomé, L. Proton beam modification of lead white pigments. *Nucl. Instrum. Methods Phys. Res. Sect. B Beam Interact. Mater. At.* **2013**, *307*, 20–24. [[CrossRef](#)]
37. Das, A.; Takahashi, Y.; Tanaki, A. Application of X-ray Absorption Fine Structure (XAFS) Spectroscopy to Speciation of Lead (Pb) Contaminants in Plastics. *Bull. Chem. Soc. Jpn.* **2015**, *88*, 341–345. [[CrossRef](#)]
38. Kabacinska, Z.; Yate, L.; Wencka, M.; Krzyminiewski, R.; Tadyszak, K.; Coy, E. Nanoscale effects of radiation (UV, X-ray, and γ) on calcite surfaces: Implications for its mechanical and physico-chemical properties. *J. Phys. Chem. C* **2017**, *121*, 13357–13369. [[CrossRef](#)]
39. Wencka, M.; Lijewski, S.; Hoffmann, S.K. Dynamics of CO_2^- radiation defects in natural calcite studied by ESR, electron spin echo and electron spin relaxation. *J. Phys. Condens. Matter* **2008**, *20*, 255237. [[CrossRef](#)]
40. Kabacińska, Z.; Krzyminiewski, R.; Tadyszak, K.; Coy, E. Generation of UV-induced radiation defects in calcite. *Quat. Geochronol.* **2019**, *51*, 24–42. [[CrossRef](#)]

Disclaimer/Publisher's Note: The statements, opinions and data contained in all publications are solely those of the individual author(s) and contributor(s) and not of MDPI and/or the editor(s). MDPI and/or the editor(s) disclaim responsibility for any injury to people or property resulting from any ideas, methods, instructions or products referred to in the content.